Vyskočilová *et al. Herit Sci* (2019) 7:26
https://doi.org/10.1186/s40494-019-0269-7

Heritage Science

RESEARCH ARTICLE Open Access

Model study of the leather degradation by oxidation and hydrolysis

Gabriela Vyskočilová[1*], Matthäa Ebersbach[2], Radka Kopecká[3], Lubomír Prokeš[3] and Jiří Příhoda[1]

Abstract

Many objects of culture heritage, comprised of leather, need to receive the right treatment to be restored and to elongate their lifespan. Determination of the degradation degree and even better the type of the degradation is a crucial knowledge for the way of subsequent conservation, exhibition and long-term storage. Collagen based materials are very sensitive to the deterioration and undergo, mainly hydrolysis and oxidation. Namely acid hydrolysis and photooxidation are the most often causes of the disintegration of leather. Contrary to the leather investigation, a few studies dedicated to parchment described some typical features of hydrolysis, oxidation and gelatinization observed applying Attenuated Total Reflection Fourier-Transform Infrared spectroscopy (ATR-FTIR) which is widely used in collagen degradation type research. Except of the collagen secondary structure, followed by IR spectroscopy, we determined the shrinkage temperature of the collagen substrate by Micro Hot Table method (MHT) to reach the degradation level. In this paper, artificially degraded leather samples as a theoretical representative of cultural heritage objects were examined. We discuss the use of both techniques (IR and MHT) as potential methods for fast assessment of oxidation and hydrolysis of vegetable tanned leathers and degradation level. New samples of leather tanned by various vegetable tannins were artificially degraded under controlled conditions. We simulated the photooxidation by means of the Xenon arc lamp exposure, oxidation using the soaking in hydrogen peroxide, acid hydrolysis by the soaking in hydrochloric acid and alkaline hydrolysis using the soaking in natrium hydroxide. ATR-FTIR spectra of reference and tested samples were compared. Oxidation causes increase of the distance between amide I (A_I) and amide II (A_{II}) wavenumbers ($\Delta\nu$) above 100 cm^{-1} and the intensity ratio between A_I and A_{II} bands (A_I/A_{II}) above 1.6. The A_I/A_{II} ratio depends on the type of hydrolysis. The increase above 1.8 proves acid hydrolysis while the decrease under 1 demonstrate alkaline hydrolysis. MHT results are not so obvious. Generally, mainly the hydrolysis causes the decrease of the temperatures. We have found out that knowledge of the whole shrinkage interval is important and provides more appropriate information about the leather disintegration.

Keywords: Leather, ATR-FTIR, MHT, Sparse PCA

Introduction

Leather, as all other materials, is disintegrated over time. However, it is hard to decide which treatment method is the best if the reason of the disintegration is unknown. That's why a method to determine the cause of the change is needed. A wide range of different effects influence the mechanism of leather deterioration. The main goal of this research was to find out useful characterization for description of leather degradation.

The main component of leather is protein called collagen. More than 28 different types of collagen exist [1]. They differ themselves by their chemical composition, molecule weight, and by content of glycosides compounds. Collagen type I is the main component of the leather. The fundamental structural units of collagen are amino acids linked through the peptide bonds to polypeptide chains. Each of peptide chain contains about 1000 amino acids residues which are divided to tripeptide segments of the repeating structure Gly–X–Y, where glycine (Gly) forms about 30%, X and Y are generally

*Correspondence: gabriela.vyskocilova@mail.muni.cz
[1] Department of Chemistry, Faculty of Science, Masaryk University, Kotlářská 267/2, 611 37 Brno, Czech Republic
Full list of author information is available at the end of the article

represented by proline (10%) and for leather characteristic amino acid hydroxyproline (10%). Arrangement of amino acids molecules into polymer molecule creates primary structure of collagen molecule, while secondary structure is related to its space orientation and it is created by left-handed α-helix or β-sheet. Three collagen α-chains form the tertiary structure—triple helical one [2–4] when different parts of the collagen molecule are held together by covalent bonds of amino groups [1, 5].

Tanning agents modify the collagen to the more stable material denoted as leather. There are different agents used for tanning. In past, the vegetable tannins (plant polyphenols) were mainly used [6]. Therefore, the present study is focused only on the vegetable tanned leather samples which are frequently found in cultural heritage collections. Vegetable tannins can be divided into two groups according to their chemical composition. Hydrolysable tannins are based on monosaccharide ring (glucose) forming gallotannins (gallic acid core) or ellagitannins (ellagic acid core). Condensed tannins are based on flavonoids [7, 8].

The most common degradation processes of collagen are oxidation, hydrolysis, and denaturation [6, 9, 10].

During the oxidation processes, collagen chain is split into shorter fragments (Fig. 1a), consisting of acid amides or keto acid derivatives. This mechanism is also connected with decrease of collagen mass weight. Especially, oxidation takes place on the basic amino acids as proline, hydroxyproline, arginine, lysine or hydroxylysine. Oxidation causes weakening of physical stability of leather [11]. The rate of this process increases at higher temperatures and lower relative humidity, light and presence of air pollutants. Vegetable tannins, undergo the oxidation process, too [6].

Liquid water contains H_3O^+ and OH^- ions that can act as both nucleophilic and electrophilic reagents that can start alkali or acidic hydrolysis of collagen [6, 9]. Peptide bonds are broken (Fig. 1b) and cause the formation of N-terminal and C-terminal residues and thus the collagen molecular weight decreases at the same time. The total hydrolysis can even lead to the formation of single amino acids. Reaction rate rises at relative humidity >70% and pH <3 (for acid hydrolysis). Vegetable tannins undergo hydrolysis, too, especially hydrolysable ones [1, 6].

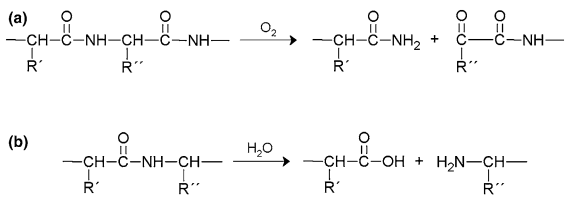

Fig. 1 Decomposition of peptide chain: **a** oxidation; **b** hydrolysis

Oxidation and hydrolysis deterioration processes can pass over separately or in combination [11].

Due to the effect of tanning agents, which leads to the formation of cross-linked bonds in collagen structure, leather has higher hydrothermal stability than hide and the shrinkage temperature (T_s) rises, too. T_s is the temperature when collagen loses its original natural structure. The leather fibres are hydrated and after subsequent continuous heating the bonds are broken and the thermal denaturation (fibres deformation) is observed as shrinkage. The denaturation is dependent on the quality of the leather itself and is characterized by degradation degree [12, 13].

In principle, there are some methods how to investigate the properties of leather. For our purposes we have chosen Micro Hot Table method (MHT). The great advantage of MHT method is using of very small sample-only 0.1 mg or several fibres are sufficient for MHT determination. Generally, MHT can be used to determine the shrinkage temperature of the leather sample [14, 15]. Therefore, this method says about deterioration degree of the leather (Table 1) [16].

Hydrothermal activity can be described by temperature intervals A, B and C. The intervals should follow in order as you can see in Fig. 2 [14, 15]. The start temperature value of the C interval corresponds with shrinkage temperature T_s. Sometimes conservators take into account only T_s during assessment of the leather, but it is necessary to observe the full shrinkage activity interval [15].

According to Larsen [16] leather substrates can be divided into five categories according their degradation level based on the T_s (Table 1).

For example, new vegetable tanned leather achieves T_s in the range of 70 to 85 °C (it depends on group of tannins) and chromed tanned leathers reach T_s over 100 °C. For comparison, T_s of the untanned hide is lower than 65 °C. T_s plays the main role in case of durability and deterioration rate: the higher T_s the higher physical–chemical stability and higher durability. The degradation processes lead to the decrease of T_s. According to previous studies [14, 15], leather is considered to be damaged if the T_s is below 60 °C. Therefore, more careful conservation approach is required. If T_s is below 45 °C, leather is

Table 1 Damage categories according to temperature range of T_s

Level of damage	T_s (°C)
1	70–90
2	60–70
3	50–60
4	40–50
5	<40

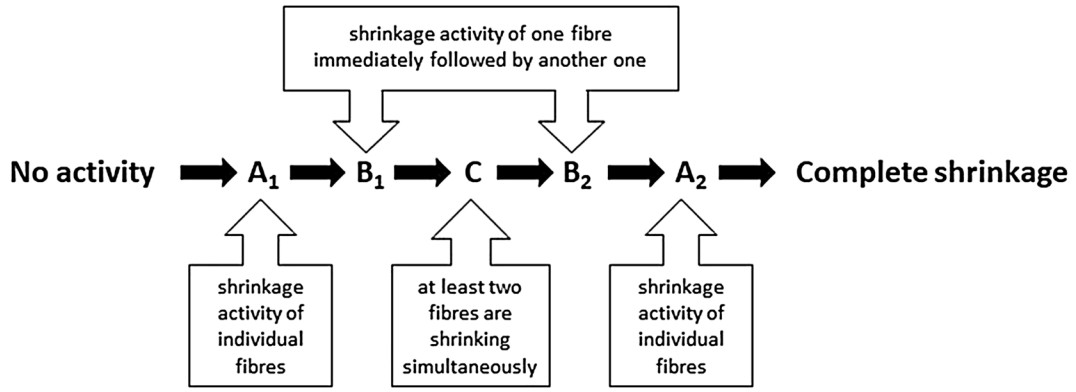

Fig. 2 The order of shrinkage intervals and their description

classified as heavily deteriorated and specific handling is necessary [6, 14, 15].

Commonly, IR spectroscopy is widely used technique for studying collagen based materials as parchment or historical and archaeological leathers [9, 17–20]. Especially, it is used for determination of their secondary and tertiary structures of proteins [21, 22]. ATR-FTIR is one of non- or semi-destructive techniques, that is helpful for investigation of valuable historical items [23, 24], in special cases taking of only small sample is possible.

The most characteristic vibrations of collagen are vibrations of amide I group (A_I) at 1630 cm^{-1} (νC=O, having the highest intensity) and the amide II group (A_{II}) at 1550 cm^{-1} (νC–N, δN–H). Their wavenumbers (Table 2) and intensities are influenced by the number of tannin–collagen bonds in leather structure Fig. 3. List of collagen and tannin characteristic wavenumbers is listed in Table 2.

Degradation affect the secondary structure of collagen [21, 22] and specific patterns can be found in the infrared spectra. These patterns have been already determined for parchment. Unfortunately, any values for leather have not been determined yet. Generally, three degradation phenomena are defined [9, 17, 28–30].

- The first one is connected with shifts of A_I and A_{II} wavenumbers. According to literature data [9, 17, 28–30], the degradation parameter $\Delta\nu(A_I–A_{II})$ is assigned to denaturation (gelatinization) process. Parchment is considered to be denatured if Δν is above 95 cm^{-1}.
- The second parameter is related to intensities of A_I and A_{II} bands, respectively to their ratio A_I/A_{II}. For

Table 2 List of the main infrared bands (cm^{-1}) of collagen tannins [25–27]

Absorption maximum (cm^{-1})	Assignment
Collagen	
~3310	Amide A: νN–H
~3080	Amide B: νN–H
~2960	νC–H
~1630	Amide I: νC=O
~1545	Amide II: νC–N, δN–H
~1450	δCH_2 of proline
~1400	δC–O–H, δNH_2
~1340	νCH_2 δC–H
~1240	Amide III: νC–N, δN–H
~1080 and 1030	νC–O, νC–O–C
Common for all tannins	
~1610	νC=C aromatic ring
~1512	νC=C aromatic ring
~1450	νC=C aromatic ring
~1210	νC–O, δC–OH
~1035	βC–H deformation, νC–O
Hydrolysable tannins	
~1705–1730	νC=O
~1320	νC–O and O–H deformation
~1085	νC–O–C
~871	γOH, γC–H
~760	γ aromatic δC–H
Condensed tannins	
~1285	νC–O pyran ring
~1160	νC–O–C
~1113	νC–O–C
~843	C–H deformation

ν, stretching; δ, bending; β, in plane; γ, out-of plane

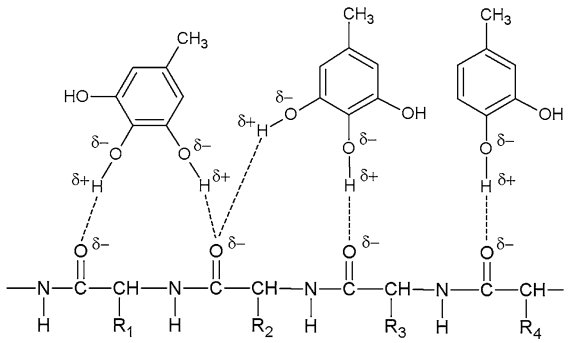

Fig. 3 Bonding of tannin molecule (**a**) to collagen structure (**b**) [1]

parchment, when the ratio A_I/A_{II} is above 1, hydrolysis should be taken account.

- For parchment, the last one is related to the appearance of new absorption band in the region 1740–1720 cm^{-1}. The occurrence of this new band shows about parchment oxidation [9, 17, 31–33]. However for leathers, the occurrence of this band is disputable at this wavenumber range, because typical bands of hydrolysable tannins can be found in this region, too.

As it was explained above, the different environmental and chemicals conditions influence changes of leather properties. Therefore, different ways of disintegration of model leather samples have been tested. We suppose that their behaviour will be similar to parchment. Therefore ATR-FTIR spectra have been recorded and shrinkage activity has been determined under altering conditions of the degradation processes that were caused by photooxidation and oxidation, acid or alkaline hydrolysis.

The purpose of this research was to explore if it is possible to use ATR-FTIR for study of leather degradation process. The determination of shrinkage activity by MHT, as technique for T_s determination, was chosen for degradation level evaluation.

Both methods are fundamental in evaluating the structural and physical–chemical changes related to ageing and deterioration of historical objects. Nowadays, they are often used for research of highly valuable historic objects. The knowledge of the type and level of degradation influence enables to choose an appropriate conservation process, e.g. choice of cleaning reagents, other conservation treatments, methods of manipulation, displaying or storage in archives and museums.

Technical equipment

The ATR-FTIR spectra were recorded in the wavenumber range of 4000–400 cm^{-1} using Bruker Tensor 27 instrument. The absorbance spectra were collected from 32 scans with a resolution of 4 cm^{-1}. The air background was read before each measurement. The data were processed using OPUS 6.5 software [34] and the spectra were corrected—the baseline was subtracted from each spectrum before data processing. The spectra of new degraded leathers (corium side) were recorded. No significant differences, between IR spectra for corium and grain side, were found after ageing.

MHT was performed on home-made equipment Melting point KEVA Boetius controlled by the temperature processor and coupled with the DinoLite digital microscope at 50× magnification. A sample of a few fibres from the corium side of the leather was wetted thoroughly with deionised water on a concave microscope slide and allowed to stand for 10 min. Afterwards, fibres were split into individual fibres, covered with cover slide and placed on the hot table of the microscope. The samples were heated at the rate 2 °C/min up to 100 °C. Each sample was measured at least twice [14, 16, 35].

Photooxidation experiments were performed using Q-SUN B02 Xenon Test Chamber at Textile Testing Institute, Brno, Czech Republic. The samples (roughly 5 × 2 cm) were exposed to xenon air cooled by arc lamp (1800 weeks) for 1 week.

Materials

The three new leather samples tanned with different tannin types (sumac, quebracho-mimosa combination and unknown tannin) were provided by Gara TZL PLUS s.r.o., Otrokovice, Czech Republic. The five new vegetable tanned leather samples (tanned with quebracho, gambier, myrobalan, mimosa and chestnut) were provided by Leather and Footwear Research Institute, Bucharest, Romania.

According to tannin agent, there are two groups of leathers–leathers containing hydrolysable tannins HL (5 samples) and condensed ones CL (4 samples).

Each sample was measured three times. All results are presented as mean values from all measurements, standard deviation S_r was calculated. It means that for HL samples the total number of measurements (n) n = 15, for CL n = 12 for each ageing method.

The list of all samples (cattle hide) is mentioned in Table 3. Sample treatment was carried out under observing ethic codex.

Degradation methods

It is necessary to mention that no similar testing of leathers has been published so far. Thus our attempt to develop a method, how to carry out experiments dealing with the leather degradation, was suggested. Similarly, no official or international standard methods, dealing with evaluation of hydrolytic or oxidative degradation, were

Table 3 List of samples and corresponding signs

Tannin group	Tannin	Reference sample	Ageing treatment					
			Xe	H_2O_2		HCl		NaOH
			1w	1w	5w	1w	5w	24 h
Hydrolysable	Sumac	$H1_{Ref}$	$H2_{Xe}$	$H1_{H_2O_2\_1w}$	$H1_{H_2O_2\_5w}$	$H1_{Hcl\_1w}$	$H1_{HCl\_5w}$	$H2_{NaOH}$
Hydrolysable	–	$H2_{Ref}$	$H2_{Xe}$	$H2_{H_2O_2\_1w}$	$H2_{H_2O_2\_5w}$	$H2_{Hcl\_1w}$	$H2_{HCl\_5w}$	$H2_{NaOH}$
Hydrolysable	Myrobalan	$H3_{Ref}$	$H3_{Xe}$	$H3_{H_2O_2\_1w}$	$H3_{H_2O_2\_5w}$	$H3_{Hcl\_1w}$	$H3_{HCl\_5w}$	$H3_{NaOH}$
Hydrolysable	Chestnut	$H4_{Ref}$	$H4_{Xe}$	$H4_{H_2O_2\_1w}$	$H4_{H_2O_2\_5w}$	$H4_{Hcl\_1w}$	$H4_{HCl\_5w}$	$H4_{NaOH}$
Hydrolysable	–	$H5_{Ref}$	$H5_{Xe}$	$H5_{H_2O_2\_1w}$	$H5_{H_2O_2\_5w}$	$H5_{Hcl\_1w}$	$H5_{HCl\_5w}$	$H5_{NaOH}$
Condensed	Quebracho + mimosa	$C6_{Ref}$	$C6_{Xe}$	$C6_{H_2O_2\_1w}$	$C6_{H_2O_2\_5w}$	$C6_{Hcl\_1w}$	$C6_{HCl\_5w}$	$C6_{NaOH}$
Condensed	Quebracho	$C7_{Ref}$	$C7_{Xe}$	$C7_{H_2O_2\_1w}$	$C7_{H_2O_2\_5w}$	$C7_{Hcl\_1w}$	$C7_{HCl\_5w}$	$C7_{NaOH}$
Condensed	Gambier	$C8_{Ref}$	$C8_{Xe}$	$C8_{H_2O_2\_1w}$	$C8_{H_2O_2\_5w}$	$C8_{Hcl\_1w}$	$C8_{HCl\_5w}$	$C8_{NaOH}$
Condensed	Mimosa	$C9_{Ref}$	$C9_{Xe}$	$C9_{H_2O_2\_1w}$	$C9_{H_2O_2\_5w}$	$C9_{Hcl\_1w}$	$C9_{HCl\_5w}$	$C9_{NaOH}$

H, hydrolysable tannins; C, condensed tannins; Ref, new non-degraded sample; Xe, photooxidation; H_2O_2, oxidation; HCl, acid hydrolysis; NaOH, alkaline hydrolysis; 1w, 1 week; 5w, 5 weeks; 24 h, 24 hours

published. The extreme conditions (e.g. the relative high concentration of reagents) were chosen to ensure degradation will be detectable and provable. The samples in one type of experiment were tested more times.

Photooxidation was performed according to description of technical equipment mentioned in chapter devoted to technical equipment.

Oxidation was performed by immersing the samples in 50 ml of 25% (v/v) H_2O_2 for 1 or 5 weeks, respectively, and placed into the darkness.

Acid hydrolyses was performed by immersing the samples in 50 ml of 25% (v/v) HCl for 1 and 5 weeks.

Alkaline hydrolysis was performed by immersing the samples in 50 ml of 10% (w/v) NaOH for 24 h.

All experiments containing liquid phase were carried out in 50 ml beaker. The size of all leather was roughly 2 × 2 cm. The beaker was covered by Parafilm®M foil.

After required time, the samples were taken out the beaker, washed with freshly distilled water until the pH of washing liquid became constant. Finally, samples were let to dry in laboratory conditions under light press.

Statistical processing

All computations were made using freely available R statistical software [36]. For principal component calculation the sparse method was considered the more suitable [37, 38].

Results and discussion

Photooxidation

Even though the photooxidation of leather samples was performed only for 1 week significant changes were observed in IR spectra in comparison with spectra of reference samples (Fig. 4).

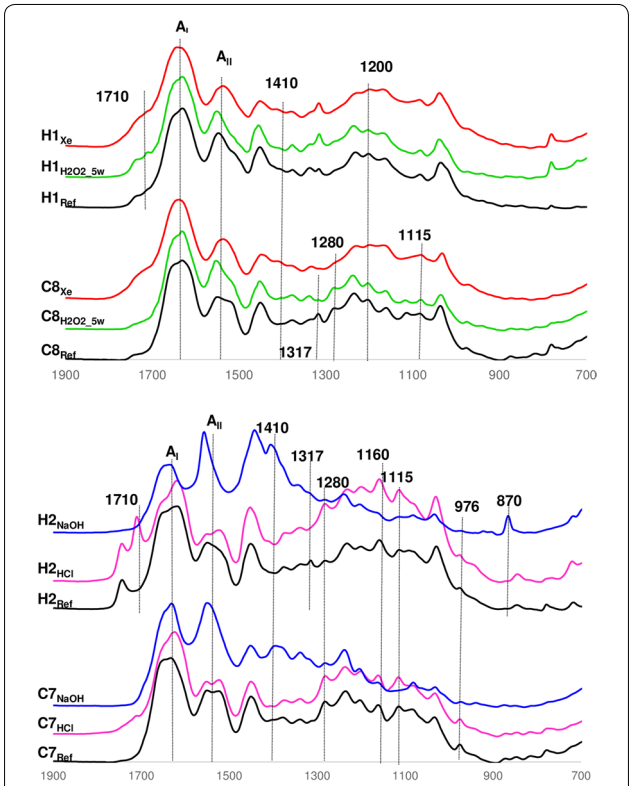

Fig. 4 ATR-FTIR spectra of leather samples

The amide peak positions (A_I a A_{II}) is comparable for both tannin groups (see Table 4 or Fig. 5). The shift of A_I to higher wavenumbers, compared with reference sample, was observed for both HL and CL tannin groups, and so $1641 \pm 5\ cm^{-1}$ for HL and $1638 \pm 3\ cm^{-1}$ for CL for 1 week treated samples (Table 4). Similarly,

Table 4 The range of observed parameters and types of degradation processes

	Hydrolysable				Condensed			
	A_I (cm^{-1})	A_{II} (cm^{-1})	$\Delta\nu(A_I-A_{II})$ (cm^{-1})	A_I/A_{II}	A_I (cm^{-1})	A_{II} (cm^{-1})	$\Delta\nu(A_I-A_{II})$ (cm^{-1})	A_I/A_{II}
Reference	1632 ± 2	1548 ± 1	85 ± 4	1.452 ± 0.104	1631 ± 1	1550 ± 1	81 ± 1	1.466 ± 0.118
Xe								
1w	1641 ± 5	1541 ± 5	100 ± 5	1.682 ± 0.151	1638 ± 3	1540 ± 3	102 ± 2	1.620 ± 0.042
H_2O_2								
1w	1632 ± 2	1549 ± 2	84 ± 3	1.451 ± 0.086	1631 ± 1	1549 ± 2	83 ± 2	1.517 ± 0.061
5w	1631 ± 2	1549 ± 2	83 ± 3	1.453 ± 0.107	1631 ± 1	1551 ± 2	81 ± 2	1.493 ± 0.094
HCl								
1w	1630 ± 2	1546 ± 3	83 ± 2	1.581 ± 0.076	1631 ± 1	1546 ± 3	85 ± 2	1.553 ± 0.068
5w	1627 ± 2	1550 ± 3	76 ± 4	1.825 ± 0.145	1628 ± 1	1551 ± 1	75 ± 3	1.842 ± 0.115
NaOH								
24h	1633 ± 2	1555 ± 2	76 ± 2	0.805 ± 0.137	1631 ± 1	1553 ± 2	80 ± 2	0.973 ± 0.120

Reference, new, non degraded samples; HCl, acid hydrolysis; NaOH, alkaline hydrolysis; H_2O_2, oxidation; Xe, photooxidation

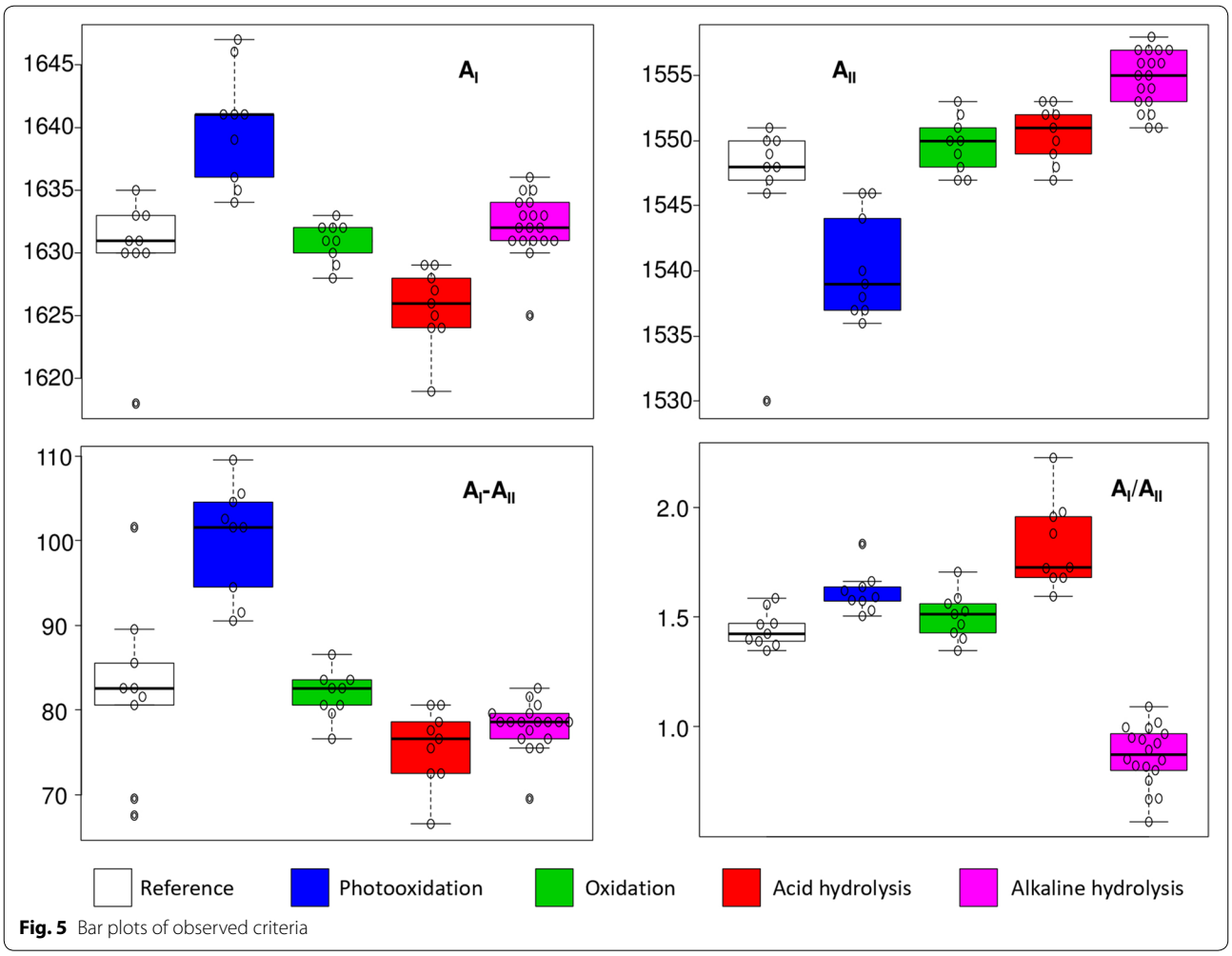

Fig. 5 Bar plots of observed criteria

Table 5 Shrinkage intervals—mean values of interval starting temperatures (°C)

	Hydrolysable						Condensed					
	A_1	B_1	C	B_2	A_2	T_{last}	A_1	B_1	C	B_2	A_2	Tl_{ast}
Ref	61.5 ± 4.3	63.6 ± 4.0	67.3 ± 5.4	74.3 ± 6.6	76.7 ± 5.0	79.1 ± 6.0	79.3 ± 0.2	81.3 ± 0.6	85.0 ± 2.2	93.6 ± 4.2	95.7 ± 4.3	96.7 ± 3.4
Xe	36.6 ± 3.2	53.4 ± 3.8	60.9 ± 9.4	72.2 ± 16.5	74.0 ± 15.2	77.9 ± 12.3	70.3 ± 6.2	73.5 ± 5.3	82.1 ± 6.0	89.3 ± 6.3	91.8 ± 6.1	92.9 ± 7.1
H_2O_2-a	63.5 ± 3.9	66.8 ± 2.4	69.8 ± 2.9	71.6 ± 4.5	79.5 ± 5.2	81.1 ± 5.4	68.5 ± 2.6	70.5 ± 2.2	74.8 ± 0.4	81.2 ± 1.2	83.0 ± 1.0	84.1 ± 0.9
H_2O_2-b	40.3 ± 1.2	43.5 ± 0.3	47.5 ± 1.0	52.9 ± 1.5	54.3 ± 1.7	57.0 ± 0.4						
HCl	47.9 ± 4.0	51.9 ± 5.9	54.1 ± 5.5	58.1 ± 4.6		60.9 ± 2.7	50.3 ± 1.6	52.1 ± 2.4	53.4 ± 2.3	58.4 ± 0.4	61.8 ± 1.2	63.9 ± 1.1

T_{last}, end of the shrinkage

the position of A_{II} was shifted, however to lower wavenumbers.

The difference Δν varies from 85 ± 4 cm^{-1} for HL_{Ref} to 100 ± 5 cm^{-1} for HL_{Xe} and from 81 ± 1 cm^{-1} for CL_{Ref} to 102 ± 2 cm^{-1} for CL_{Xe} (Table 4). Results are comparable with literature data [9, 17], dedicated to parchment where the increase of the Δν above 95 cm^{-1} can be ascribed to gelatinization.

Due to the influence of light, intensity of A_{II} decreased. Therefore, the ratio of A_I/A_{II} increased after the exposure of leather samples (Fig. 5).

As was mentioned in "Introduction", generally, the oxidation of parchment is characterized by appearance of new absorption band at 1740–1720 cm^{-1}. In our experiments, the formation of such band was not observed (Fig. 4).

Moreover, some other changes in IR spectra were observed, such as decrease of intensity even disappearance of typical bands of collagen and tannin bands at ~ 1317 (tannins $C7_{Xe}$, $C8_{Xe}$, $C9_{Xe}$), ~ 1280 (condensed tannins, $H2_{Xe}$, $C6_{Xe}$, $C7_{Xe}$, $C8_{Xe}$, $C9_{Xe}$), ~ 1200 (tannins $H2_{Xe}$, $H4_{Xe}$, $C6_{Xe}$,), ~ 1114 (condensed tannins $H2_{Xe}$, $H4_{Xe}$, $C6_{Xe}$, $C7_{Xe}$, $C8_{Xe}$, $C9_{Xe}$) and 976 cm^{-1} (condensed tannins $H4_{Xe}$, $C6_{Xe}$, $C7_{Xe}$, $C8_{Xe}$) (Fig. 4).

On the other hand, shoulder or weak band at 1412 cm^{-1} ($H2_{Xe}$, $H4_{Xe}$, $H5_{Xe}$ $C6_{Xe}$, $C7_{Xe}$, $C8_{Xe}$, $C9_{Xe}$) was found. The vibration band at ~ 1412 cm^{-1} is assigned to the bending vibration of C–OH group coming from photooxidation of carboxylic acid [25–27].

As it was mentioned above, the hydrothermal stability can be described by several intervals (Fig. 2).

As regard temperatures in interval A_1, reference samples had starting temperature at 61.5 ± 4.3 °C for HL (Table 5), while values for photooxided HL samples decreased extremely to 36.6 ± 3.2 °C (Fig. 6). All mean values of start interval temperatures are listed in Table 5.

The start temperature values of the B_1 interval for aged samples (Fig. 6) were lower than values for reference ones of both tannin groups (Table 5). Reference samples reached temperature 79.3 ± 0.2 °C, the values for photodegraded samples were not too different (70.3 ± 6.2 °C).

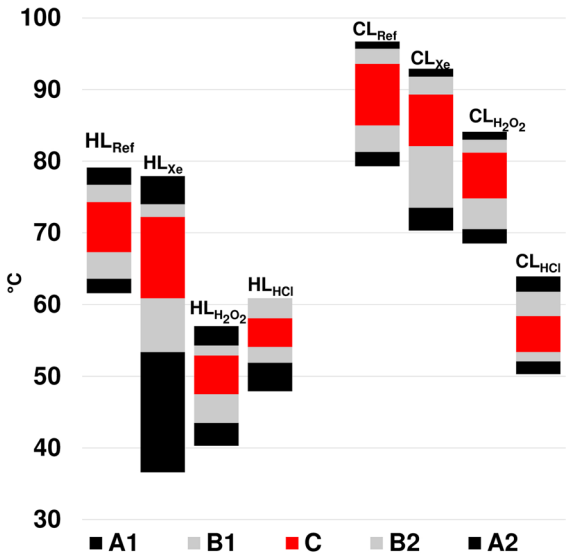

Fig. 6 MHT—development of the shrinkage intervals according to degradation process (°C), based on mean value

As regard interval C, reference leather samples, tanned by hydrolysable tannins, reached generally lower T_s values (67.3 ± 5.4 °C) than leathers tanned by condensed tannins (85.0 ± 2.2 °C) which is in agreement literature data [39]. T_s for photooxidized samples decreased mainly in case of HL group (from 67.3 ± 5.4 °C to 60.9 ± 9.4 °C) while CL changed only from 85.0 ± 2.2 °C for reference to 82.1 ± 6.0 °C for photooxided.

The temperature values for reference and degraded samples in A_2 an B_2 intervals were almost identical (Table 5).

It follows from the results mentioned above that leathers tanned by hydrolysable tannins are more susceptible to photooxidation than leathers tanned by condensed tannins, which was proved by lower values of start temperatures for intervals A_1, B_1 and C. According to above mentioned classification, the leather samples HL_{Ref} and

HL_{Xe} fall into the category 2 (Table 1). Samples CL_{Ref} and CL_{Xe} fall into category 1.

In accordance with previous investigations [14, 15, 24, 40], leather is more susceptible to photooxidation than parchment—significant changes in IR spectra after 1 week of ageing were observed (Fig. 4). The greater susceptibility of leather can be explained by the presence of tannin and its faster degradation. It follows from evaluation of all results that photooxidation is characterized by the shift of the A_I band to a higher wavenumber. A_{II} position moves to a lower wavenumbers. Consequently, the Δν value increases over 100 cm^{-1} and the ratio A_I/A_{II} is greater than 1.6 at the same time which indicates the photooxidation. Moreover, new band at ~ 1412 cm^{-1} appeared in IR spectra and some bands are dismissed or weakened (~ 1317, 1280, 1200, 1114 and 976 cm^{-1}).

As was mentioned in "Introduction" T_s (the beginning of C interval) is often used by conservators for evaluation of leather degradation. But it is necessary to follow the course of all intervals (from A_1 to T_{last}), as in this case. Photooxidation has greater influence on intervals A_1, B_1, while T_s (start temperature of interval C) is not too influenced by photooxidation. Photooxidation occur influence on the hydrothermal stability of leather samples. It can be postulated that hydrolysable tanned leathers are affected more than condensed tanned ones.

Oxidation

Character of ATR-FTIR measurements did not prove any significant structural changes in the leather (Figs. 4, 5). But evident changes were found studying hydrothermal stability of samples after 5 weeks ageing cycle (Table 5). In case of CL_{5w}, all intervals are approximately about 10 °C lower than values for reference samples (Fig. 6). The A_1 of $CL_{H_2O_2\_5w}$ samples started at 68.5 ± 2.6 °C, while references was 79.3 ± 0.2 °C, T_s decreased from 85.0 ± 2.2 °C to 74.8 ± 0.4 °C and T_{last} decreased from 96.7 ± 3.4 °C to 84.1 ± 0.9 °C (Table 5).

Different behaviour was observed for samples tanned by hydrolysable tannins. They can be distinguished into two groups. The values in the first group "a" (samples $H2_{H_2O_2\_5w}$ and $H3_{H_2O_2\_5w}$) were comparable with reference values (Table 5). The second group "b" (samples $H1_{H_2O_2\_5w}$, $H4_{H_2O_2\_5w}$, $H5_{H_2O_2\_5w}$) had corresponding values significantly lower than reference ones (Fig. 6). For instance, A_1 decreased up to 40.3 ± 1.2 °C while reference value was 61.5 ± 4.3 °C, T_s decreased to 47.5 ± 1 °C, reference value was 67.3 ± 5.4 °C and T_{last} was 57.0 ± 0.4 °C for aged one (reference reached 79.1 ± 6.0 °C). All results are listed in Table 5.

According to Table 1, samples $CL_{H_2O_2}$ still fall into the category 1 while the samples in group $HL_{H_2O_2\ -\ b}$ fall into the category 4.

Results show that leather soaked for 5 weeks in H_2O_2 was not disintegrated, as regard the secondary collagen structure, because almost any significant or typical patterns of degradation were not found (Fig. 5). Just slightly more intensive shoulder at 1740–1710 cm^{-1} was observed in case of samples $H1_{H_2O_2\_5w}$ (Fig. 4) and $H2_{H_2O_2\_5w}$. If we take account the behaviour of parchment in similar conditions [9, 17], appearance of this new bands in IR spectra is ascribed to oxidation. Unfortunately, hydrolysable tannins absorb IR irradiation in this region, too, and thus this result can be hardly interpreted.

Acid hydrolysis

Acid hydrolysis can often cause very dangerous leather degradation. This process is typical for leathers because acid gases (SO_2, NO_X) and corresponding acids, respectively, are formed in the atmosphere [6].

It follows from Table 4, that the wavenumber of A_I was slightly shifted to lower values in the dependence on time of soaking a sample by HCl solution. Values are almost identical for hydrolysable and condensed tanned leathers.

Further, the wavenumber of A_{II} was almost without changes after 1 week of ageing. The A_{II} wavenumbers after 1 week of ageing (1546 ± 3 cm^{-1}) were almost the same for both tannins groups. The similar values were also reached after 5 weeks of ageing Table 4.

The small differences in A_I and A_{II} have only little impact on Δν. The change of Δν value was negligible after the first week of ageing (HL_{Ref} 85 ± 4 cm^{-1} and HL_{HCl_1w} 83 ± 2 cm^{-1}). Only small increase was found for CL group (CL_{Ref} was 81 ± 1 cm^{-1} and 85 ± 2 cm^{-1} for CL_{HCl_1w}). The Δν decrease after 5 weeks of aging was observed (Fig. 5) for HL_{HCl_5w} (76 ± 4 cm^{-1}) and for CL_{HCl_5w} (75 ± 3 cm^{-1}) (Table 4).

For acid hydrolysis, the most remarkable changes were found at the intensity of A_{II} that reflect the A_I/A_{II} (HL_{Ref} 1.452 ± 0.104, HL_{HCl_1w} 1.581 ± 0.076; CL_{Ref} 1.466 ± 0.118, CL_{HCl_1w} 1.517 ± 0.068) after first week of ageing. Significant change of $A_{II}$was observable after 5 weeks (Fig. 5) of ageing (HL_{HCl_5w} 1.825 ± 0.145, CL_{HCl_5w} 1.842 ± 0.115) (Table 4). Results are comparable for hydrolysable and condensed tanned leathers and practically no significant difference, as consequence of the type of tannin, was found. It is quite unexpected because the greater deterioration could be awaited in case of hydrolysable tannins. It can be caused by relatively drastic acid conditions.

The tannin band at ~ 1315 cm^{-1} present at sample $H1_{Ref}$, $H2_{Ref}$, $C8_{Ref}$ and $C9_{Ref}$ dismissed or the intensity

decreased after degradation (Fig. 4). It affirms the fact that tannins are degraded in acid conditions, too.

Newly, the shoulder or band at ~1710 cm^{-1} was observed (Fig. 4) in case of all leather samples. This band was most evident in sample $H2_{HCl\_5w}$. The resolution and intensity of vibration bands increased with longer time of soaking. Moreover, small shoulder at ~1410 cm^{-1} was observed at all samples, mainly in HL samples $H2_{HCl\_5w}$, $H4_{HCl\_5w}$ and $H5_{HCl\_5w}$.

It can be said that acid hydrolysis plays important role in the hydrothermal stability at both tannin groups. Evaluation of the start temperature values of all intervals after 5 weeks of ageing leads to the conclusion that they are comparable and very similar for HL and CL (e.g. A_1 of the $HL_{HCl\_5w} = 47.9 \pm 4.0$ °C and $CL_{HCl\_5w} = 50.3 \pm 1.6$ °C; T_s is 51.9 ± 5.5 °C for HL_{HCl_5w} and 53.4 ± 2.3 °C for CL_{HCl_5w}; T_{last} reached 60.9 ± 2.7 °C for HL_{HCl_5w} and 63.9 ± 1.1 °C for CL_{HCl_5w}). All results are summarized in Table 5. After 5 weeks of degradation, all samples fall into the category 3 (Table 1), does not matter tannin group.

It follows from results that the corresponding Δν value can be used for detection of acid hydrolysis (Fig. 5). The Δν of our samples decrease below 75 cm^{-1} and then leathers are predisposed to easier gelatinization that was also confirmed by MHT. Acid hydrolysis can be also proved by ratio A_I/A_{II}, which increases over 1.8. Moreover, new band or shoulder at ~1710 cm^{-1} and small shoulder at ~1410 cm^{-1} were detected after acid hydrolytic degradation process. On the contrary to that, the band at ~1315 cm^{-1} dismissed.

Alkaline hydrolysis

Alkaline hydrolysis was performed by immersing leather samples into 10% NaOH for 24 h (if the samples had been immersed longer or the NaOH concentration was higher, the leather became very fragile). Using of 10% solution was chosen to be sure that the leather deterioration will be evident whereas corium and grain layer were not possible to distinguish, neither visually nor microscopically.

No changes in A_I wavenumber were observed. After ageing, wavenumbers were similar for both tannin groups (Table 2) but the shape and intensity of bands were changed significantly. The shape of A_I and A_{II} bands were more symmetrical after degradation (Fig. 4).

The position of A_{II} is shifted to higher wavenumbers, especially in case of HL (reference value 1548 ± 1 cm^{-1} and 1555 ± 2 cm^{-1} after alkaline hydrolysis). Negligible shift was found for CL_{Ref} (1550 ± 1 cm^{-1}), after alkaline hydrolysis the value was 1553 ± 2 cm^{-1}. Small shift of A_{II} influenced consequently the Δν value which decreased especially for hydrolysable tanned samples from HL_{Ref} 85 ± 4 cm^{-1} to 76 ± 2 cm^{-1} for HL_{NaOH}. Insignificant changes were found for CL samples (CL_{Ref} was 81 ± 1 cm^{-1} and 80 ± 2 cm^{-1} for CL_{NaOH}) (Table 4).

For all samples, the intensity of A_I decreased (Fig. 5) while intensity of A_{II} is much higher.

The huge increase of A_{II} intensity is inspectional mainly for hydrolysable samples $H1_{NaOH}$, $H2_{NaOH}$, $H4_{NaOH}$, $H5_{NaOH}$ and $C6_{NaOH}$. It can be said that this A_{II} intensity increase is the most characteristic demonstration of alkaline hydrolysis. However in some cases, the A_{II} intensity is comparable with A_I intensity for samples $C7_{NaOH}$, $C8_{NaOH}$ and $C9_{NaOH}$ (Fig. 4).

Therefore it is not surprising that the A_I/A_{II} ratio was totally reversed. The samples HL_{NaOH} have the A_I/A_{II} ratio 0.805 ± 0.137 and CL_{NaOH} (0.973 ± 0.120) (Table 4).

Weakening or disappearance of characteristic tannin bands at ~1744 ($H1_{NaOH}$, $H2_{NaOH}$), ~1317 ($H2_{NaOH}$, $H3_{NaOH}$, $C8_{NaOH}$, $C9_{NaOH}$), ~1280 ($H2_{NaOH}$, $H3_{NaOH}$,$C7_{NaOH}$, $C9_{NaOH}$), ~1160 and 1115 ($H2_{NaOH}$, $H4_{NaOH}$, $C7_{NaOH}$, $C8_{NaOH}$ and $C9_{NaOH}$), ~976 cm^{-1}($H2_{NaOH}$, $H3_{NaOH}$, $H4_{NaOH}$, $C7_{NaOH}$) supports the tannin degradation (Fig. 4).

On the other hand, new weak bands at ~1410 cm^{-1} was found in all degraded samples and intensive band ~870 cm^{-1} was detected in case of samples $H1_{NaOH}$, $H2_{NaOH}$, $H4_{NaOH}$, $C8_{NaOH}$, $C9_{NaOH}$) (Fig. 4). The band at ~870 cm^{-1} is assigned to C–H or C–C vibration and can be ascribed to the chain splitting.

After course of alkaline hydrolysis, the samples became very brittle. Therefore, it was not possible to separate fibres from samples for MHT determinations. Moreover, it was also not possible to recognize grain and corium side.

Our results indicate that the leathers, tanned by hydrolysable tannins HL, are more sensitive to alkaline hydrolysis than leathers tanned by condensed tannins CL. The proof is decrease of Δν under 76 cm^{-1} for HL while for CL the Δν value was almost identical with reference sample (Table 4).

The fact, that intensities of both amides A_I, A_{II} are swapped and the ratio A_I/A_{II} is below value 1, denotes that leather samples underwent alkaline hydrolysis (Fig. 5).

Statistical processing

For principal components calculation more suitable sparse method [37, 38] was used (library *sparsepca*).

Based on scree plot, three important principal components (PC1 53.4%; PC2 29.1% and PC3 7.1%) cover almost 90% of the total variability, were identified (Additional file 1: Fig. S1).

It follows from Fig. 7a that only photooxided samples are distinguishable according to positive values of PC1. In the Fig. 7a, acid and alkaline hydrolysed samples were

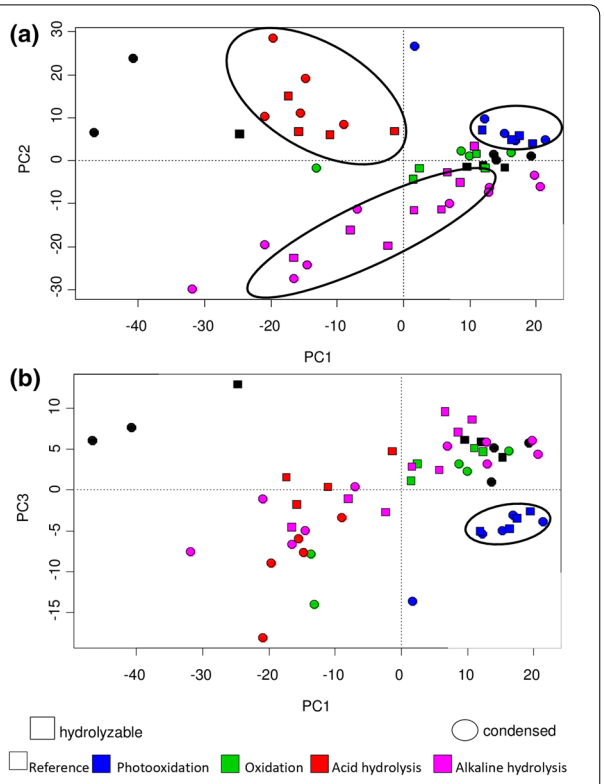

Fig. 7 Score plot (**a** PC1 vs PC2; **b** PC1 vs PC3) of IR spectra

distinguished by PC2 values: for acid hydrolysis positive values and alkaline hydrolysis negative values of PC2 were found.

Photooxided samples were distinguished more precisely (Fig. 7b) from the other degradation patterns if the PC1 and PC3 were combined.

If the PC2 and PC3 values were combined (Additional file 1: Fig. S2), alkaline and acid hydrolysis samples were distinguishable due to their PC2 values. Acid hydrolysis samples had positive values of PC2 whereas samples treated with alkaline hydrolysis fell into negative values of PC2. Similarly as in the two cases above, photooxidation was the best distinguishable.

It was also possible to recognize specific regions of spectra based on PC1 loading plots (Additional file 1: Fig. S3). Positive values correspond to photooxidation and oxidation of hydrolysable tanned samples. These results were comparable with the above discussed gains where the new absorption band in region 1800–1700 cm^{-1} was identified. It is possible to distinguish between photooxidation and oxidation due to PC3 loadings plot (Additional file 1: Fig. S4). The values corresponding photooxidation were in positive part of the plot, whereas oxidation was proven in negative part of the loading plot. The region 1800–1700 cm^{-1} in negative part of the plot corresponds to photooxidation pattern mentioned above. In case of oxidation no spectral changes were observed (see "Oxidation" section) but in the PCA loading plot some changes can be occurred in region 1500 cm^{-1} and 1150–1000 cm^{-1}.

Acid and alkaline hydrolyses were distinguishable with using of PC2 loading plot (Additional file 1: Fig. S5) when the acid hydrolysis was proved in positive part of the loading plot whereas alkaline hydrolysis was occurred in its negative part. For alkaline hydrolysis were important regions around 1550–1400 cm^{-1} and 900 cm^{-1} what was in agreement with IR spectra results mentioned in the chapter "Alkaline hydrolysis". There was proved new vibrational band at 1400 cm^{-1} and 870 cm^{-1}. On the other hand, acid hydrolysis was detected in the PC2 loading plot (Additional file 1: Fig. S5) in regions around 1800–1700 cm^{-1} and 1200–900 cm^{-1}. The first region is in agreement with the spectra, where the occurrence of new absorption band was observed around 1710 cm^{-1}. However, no significant changes for acid hydrolysis were observed for comparison of the spectra in the region 1200–900 cm^{-1}.

If the AI and AII wavenumbers were put together into the plot (Additional file 1: Fig. S6) only the alkaline hydrolysis was separated in region 1632 cm^{-1} for A_I and 1556 cm^{-1} for A_{II}. In the same plot, the highest wavenumber for A_I 1640 cm^{-1} and more, and the lowest wavenumber for A_{II} (under 1545 cm^{-1}) were found for photooxidation.

When the A_{II} and $\Delta\nu$ were put together (Additional file 1: Fig. S7), photooxidation came to wavenumber of A_{II} were under 1545 cm^{-1} and the $\Delta\nu$ was up to 90 cm^{-1}. Similarly alkaline hydrolysis of condensed tanned leathers was distinguishable when A_{II} wavenumber was 1555 cm^{-1} or higher and the $\Delta\nu$ was between 75 and 80 cm^{-1}.

When the A_I wave number and the A_I/A_{II} values were compared (Additional file 1: Fig. S8), the alkaline hydrolysis was proven for A_I between 1630 and 1653 cm^{-1} together with the A_I/A_{II} ratio less than 1.2. In the same plot photooxidation was detect for the A_I wavenumbers higher than 1635 cm^{-1} and the A_I/A_{II} ratio around 1.6. It was also possible to distinguish the acid hydrolysis for the A_I wavenumbers between 1624 and 1628 cm^{-1} and the A_I/A_{II} higher than 1.5.

Comparison of the A_{II} wavenumber and the A_I/A_{II} ratio also enable to distinguish the alkaline hydrolysis very well (Fig. 8a). The A_{II} position was around 1550–1560 cm^{-1} with the A_I/A_{II} ratio under 1.2. Similarly, the photooxidation was distinguishable when A_{II} was between 1535 and 1545 cm^{-1} and the A_I/A_{II} ratio was from 1.5 to 1.6.

It follows from Fig. 8b that photooxidation was determined when $\Delta\nu$ is 100–110 cm^{-1} and the A_I/A_{II} ratio is 1.5–1.8. Acid hydrolysis is detected when $\Delta\nu$ is

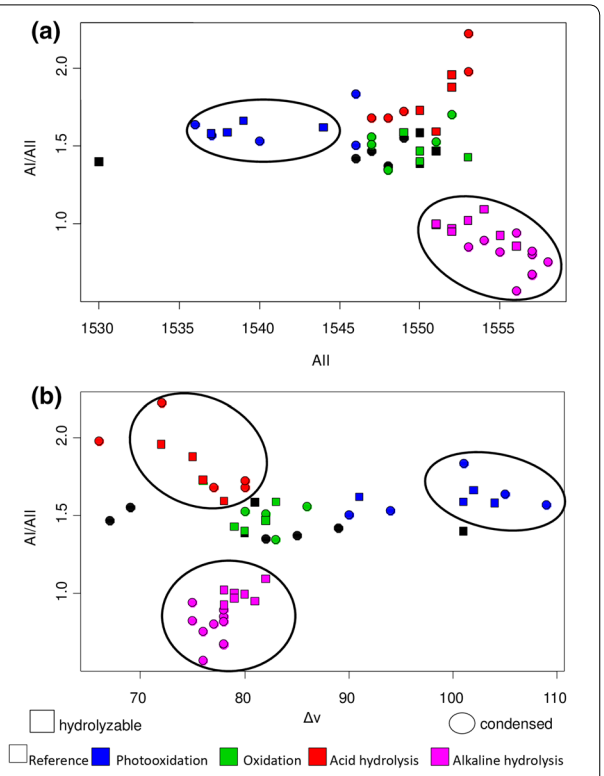

Fig. 8 Plot of A_{II} wavenumber vs A_I/A_{II} ratio (**a**), Δν vs A_I/A_{II} (**b**)

70–80 cm^{-1} and the A_I/A_{II} was higher than 1.5. Finally, the alkaline hydrolysis was distinguishable when Δν was between 75 and 82 and the A_I/A_{II} was lesser than 1.2.

Above mentioned results were summarized using classification and regression tree (CART) model [41, 42]. The calculation was made with R-libraries *rpart* and *rpart.plot*. As was determined, for alkaline hydrolysis the A_I/A_{II} ratio was lower than 1, in the CART model indicate this threshold value same degradation type under 1.2 (Fig. 9). On the other hand, photooxidation was determined when the position of A_I was shifted under 1634 cm^{-1} by both methods—the scatter plots and the CART model.

Conclusion

Some important patterns for degradation changes of leather were observed for most types of degradation processes. Photooxidation was demonstrated by increase of amide bands distance $\Delta\nu(A_I–A_{II})$ which was more than 100 cm^{-1} and increase of amide band intensities ratio A_I/A_{II} more than 1.6. The newly created band at 1730–1710 cm^{-1} can be misinterpreted as the evidence of hydrolysable tannins and it is necessary to take a cautious approach. On the other hand, both type of hydrolyses caused decrease of the distance Δν that is then less than 76 cm^{-1}, generally. The change of amides ratio A_I/A_{II} is

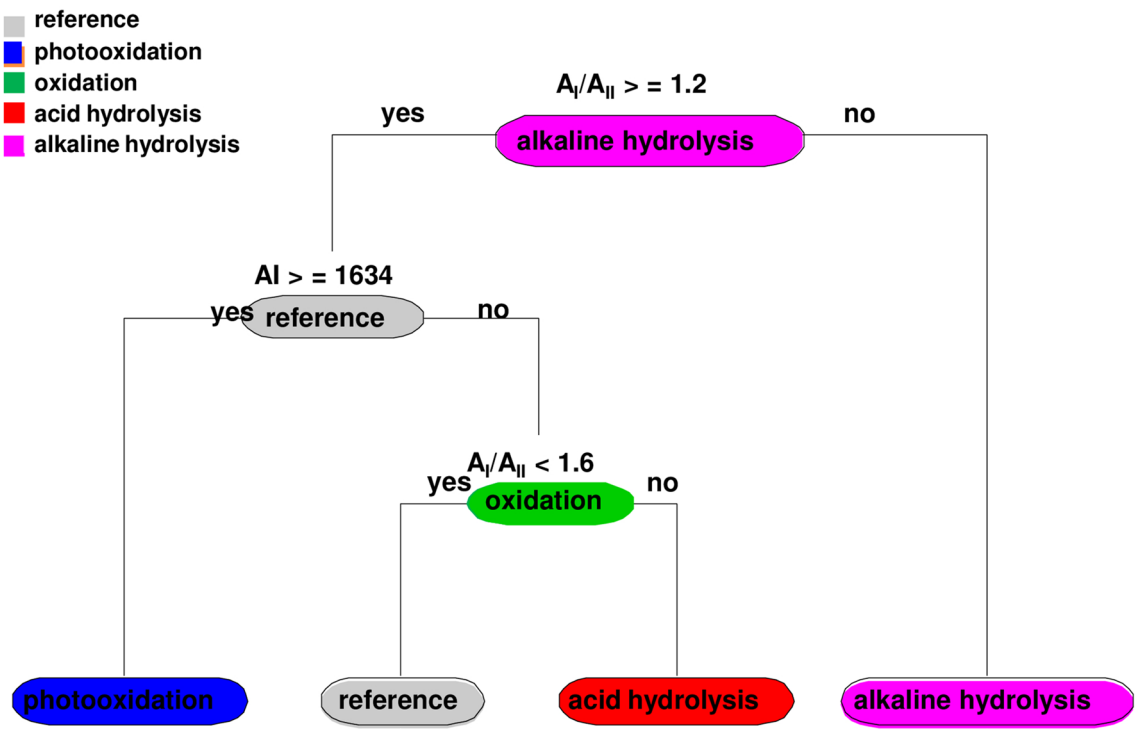

Fig. 9 Classification tree

not definite because acid hydrolysis causes the increase over 1.8 while alkaline hydrolysis caused decrease of the same ratio even less than 1. The common conclusion for both type of hydrolyses was disappearing of band at ~1315 cm^{-1}. However, some bands are created newly (~1720, ~1410 or ~870 cm^{-1}) or disappeared (~1114 and ~976 cm^{-1}) during all types of disintegration. That is why it is not possible to use it for specific determination of degradation process, but it is possible to use them for general evaluation.

As it was published earlier [14, 24, 43], the determination of hydrothermal stability, namely T_s, determined by MHT method, is useful for evaluation of historical leathers and parchment. Unfortunately, it is not appropriate to recognize type of degradation. Results show that not only T_s is the important value. It is needed to take all activity interval account as was observed in this study, too. Especially in case of photooxidation, samples had significantly lower beginning of interval A_1 an B_1. Acid hydrolysis influenced all shrinkage intervals when. The results affirmed how important the determination of T_s is.

Statistical processing affirmed results

The deeper determination of more specific borders of degradation pathways using ATR-FTIR technique and MHT method would allow to assessment of degradation degree of leather more precisely. Moreover, the behaviour of leather in real environment should be also investigated.

Additional file

Additional file 1. Additional figures.

Abbreviations

ATR-FTIR: Attenuated Total Reflection Fourier-Transform Infrared spectroscopy; MHT: Micro Hot Table method; A_I: amide I; A_{II}: amide II; T_s: shrinkage temperature; A_1: interval A_1; B_1: interval B_1; C: interval C; B_2: interval B_2; A_2: interval A_2; T_{last}: end of the shrinkage; HL: group of hydrolysable tanned leather; CL: group of condensed tanned leathers; H: hydrolysable tannins; C (as name of sample): condensed tannins; P: parchment; Ref: reference = new non-degraded sample; Xe: photooxidation; H_2O_2: oxidation; HCl: acid hydrolysis; NaOH: alkaline hydrolysis; 1w: 1 week; 5w: 5 weeks; 24h: 24 h; v: stretching; δ: bending; β: in plane; γ: out-of plane; HL: hydrolysable tanned leather samples; CL: condensed tanned samples; Sr: standard deviation.

Authors' contributions

GV and ME have carried literature study, all FTIR and MHT analyses and their evaluation, LP has processed PCA analysis. JP, RK and GV did final sequence alignment in the manuscript and drafted manuscript. All authors read and approved the final manuscript.

Author details

[1] Department of Chemistry, Faculty of Science, Masaryk University, Kotlářská 267/2, 611 37 Brno, Czech Republic. [2] Faculty of Agriculture/Environment/Chemistry, Hochschule für Technik und Wirtschaft Dresden, Dresden, Germany. [3] Department of Chemistry and Department of Physical Electronics, Faculty of Science, Masaryk University, Kotlářská 267/2, 611 37 Brno, Czech Republic.

Acknowledgements

To Textile Testing Institute, Brno, (CZ) and The National Research and Development Institute for Textiles and Leather–Leather and Footwear Research Institute, Bucharest, (RO).

Competing interests

The authors declare that they have no competing interests.

Availability of data and materials

The datasets used and/or analysed during the current study are available from the corresponding author on reasonable request.

Funding

MUNI/A/1288/2017.

Publisher's Note

Received: 12 December 2018 Accepted: 25 April 2019
Published online: 11 May 2019

References

1. Covington T. Tanning chemistry : the science of leather. Cambridge: Royal Society of Chemistry; 2009. p. 550.
2. Kadler KE, Holmes DF, Trotter JA, Chapman JA. Collagen fibril formation. Biochem J. 1996;316:1–11.
3. Brodsky B, Ramshaw JAM. The collagen triple-helix structure. Matrix Biol. 1997;15:545–54.
4. Mühlen Axelsson K, Larsen R, Sommer DVP. Dimensional studies of specific microscopic fibre structures in deteriorated parchment before and during shrinkage. J Cult Herit. 2012;13(2):128–36.
5. Gelse K, Pöschl E, Aigner T. Collagens—structure, function, and biosynthesis. Adv Drug Deliv Rev. 2003;28:1531–46.
6. Kite M, Thomson R. Conservation of leather and related materials. Oxford: Butterworth-Heinemann; 2006. p. 340.
7. Hagerman AE. Tannin Handbook Oxford OH 45056: Miami University; 2011. http://www.users.muohio.edu/hagermae/.
8. Falcao L, Araujo MA-O. Vegetable tannins used in the manufacture of historic leathers. Molecules. 2018;23(5):20.
9. Ciglanská M, Jančovičová V, Havlínová B, Machatová Z, Brezová V. The influence of pollutants on accelerated ageing of parchment with iron gall inks. J Cult Herit. 2014;15(4):373–81.
10. de Groot J. Damage assessment of parchment with scanning probe microscopy [PhD thesis]. Birkbeck: University of London; 2007.
11. Larsen R. The chemical degradation of leather. CHIMIA Int J Chem. 2008;62(11):899–902.
12. Mühlen AK, Larsen R, Sommer D, Melin R. Establishing the relation between degradation mechanisms and fibre morphology at microscopic level in order to improve damage diagnosis for parchments: a preliminary study. In: ICOM-CC 18th triennial conference. Copenhagen, Denmark. 2017. p. 9.
13. Larsen R, Poulsen DV, Minddal K. Damage of parchment fibres on the microscopic level detected by the micro hot table (MHT) method. In: Larsen R, editor. Improved damage assessment of parchment (IDAP): assessment, data collection and sharing of knowledge, research report

No 18. Copenhagen: The Royal Danish Academy of Fine Arts; 2007. p. 69–72.
14. Larsen R, Vest M, Bøgvad Kejser U. STEP Leather Project : evaluation of the correlation between natural and artificial ageing of vegetable tanned leather and determination of parameters for standardization of an artificial ageing method. København: Royal Danish Academy of Fine Arts; 1994. p. 180.
15. Larsen R. ENVIRONMENT Leather Project : deterioration and conservation of vegetable tanned leather. København: Royal Danish Academy of Fine Arts, School of Conservation; 1996.
16. Larsen R, Sommer D, Mühlen Axelsson K. Scientific approach in conservation and restoration of leather and parchment objects in archives and libraries. In: Engel P, editor. New approaches to book and paper conservation-restoration. Horn/Wien: Verlag Berger; 2011. p. 239–58.
17. Carşote C, Budrugeac P, Decheva R, Haralampiev NS, Miu L, Badea E. Characterization of a byzantine manuscript by infrared spectroscopy and thermal analysis. Rev Roum Chim. 2014;59(6–7):429–36.
18. Zhang Y, Chen Z, Wang C, Tian Y, Gong D. Studies of structure changes of archeological leather by FTIR spectroscopy. J Soc Leather Technol Chem. 2018;102(5):262–7.
19. Bicchieri M, Monti M, Piantanida G, Pinzari F, Sodo A. Non-destructive spectroscopic characterization of parchment documents. Vib Spectrosc. 2011;55:267–72.
20. Carsote C, Kövari L, Albu C, Hadîmbu E, Badea E, Miu L, et al. Bindings of rare books from the collections of the Romanian Academy Library—a multidisciplinary study. Leather Footwear J. 2018;18:307–20.
21. Stuart B. Infrared spectroscopy. Fundamentals and applications. New York: Wiley; 2004.
22. Barth A. Infrared spectroscopy of proteins. Biochim Biophys Acta. 2007;1767:1073–101.
23. Sendrea C, Carsote C, Badea E, Adams A, Niculescu M, Iovu H. Non-invasive characterisation of collagen-based materials by NMR-mouse and ATR-FTIR. University Politehnica of Bucharest Scientific Bulletin Series B-Chemistry and Materials Science. 2016;78(3):27–38.
24. Larsen R. Improved damage assessment of parchment (IDAP): assessment, data collection and sharing of knowledge. [Luxembourg]: European Commission, Directorate-General for Research, Directorate I-Environment; 2007.
25. Ricci A, Olejar KJ, Parpinello GP, Kilmartin PA, Versari A. Application of fourier transform infrared (FTIR) spectroscopy in the characterization of tannins. Appl Spectrosc Rev. 2015;50(5):407–42.
26. Falcao L, Araujo MEM. Application of ATR-FTIR spectroscopy to the analysis of tannins in historic leathers: the case study of the upholstery from the 19th century Portuguese Royal Train. Vib Spectrosc. 2014;74:98–103.
27. Boyatzis SC, Velivasaki G, Malea E. A study of the deterioration of aged parchment marked with laboratory iron gall inks using FTIR-ATR spectroscopy and micro hot table. Herit Sci. 2016;4(1):13.
28. Badea E, Miu L, Budrugeac P, Giurginca M, Mašić A, Badea N, et al. Study of deterioration of historical parchments by various thermal analysis techniques complemented by SEM, FTIR, UV–Vis–NIR and unilateral NMR investigations. J Therm Anal Calorim. 2008;91(1):17–27.
29. Plavan V, Giurginca M, Budrugeac P, Vilsan M, Miu L. Evaluation of the physico-chemical characteristics of leather samples of some historical objects from kiev. Rev Chim. 2010;61(7):627–31.
30. Carsote C, Miu L, Petroviciu I, Creanga DM, Giurginca M, Vetter W. Scientific investigation of leather in ethnographical objects by molecular spectroscopy and MHT2012. p. 183–92.
31. Branden C, Tooze J. Introduction to protein structure. New York: Garland Science; 1999. p. 410.
32. Belbachir K, Noreen R, Gouspillou G, Petibois C. Collagen types analysis and differentiation by FTIR spectroscopy. Anal Bioanal Chem. 2009;395(3):829–37.
33. Derrick MR, Stulik D, Landry JM. Infrared spectroscopy in conservation science. Los Angeles: Getty Conservation Institute; 1999. p. 248.
34. OPUS 6.5 software.
35. Budrugeac P, Miu L, Souckova M. The damage in the patrimonial books from Romanian libraries: thermal analysis methods and scanning electron microscopy. J Therm Anal Calorim. 2007;88(3):693–8.
36. R Studio. https://cran.r-project.org/.
37. Zou H, Hastie T, Tibshirani R. Sparse principal component analysis. J Comput Grap Stat. 2006;15(2):265–86.
38. Zou H, Xue L. A selective overview of sparse principal component analysis. Proc IEEE. 2018;106(8):1311–20.
39. Kite M, Thomson R. Conservation of leather and related materials. Oxford: Butterworth-Heinemann; 2006. p. 368.
40. Petroviciu I, Carsote C, Wetter W, Miu L, Shreiner M, editors. Artificially aged parchment investigated by FTIR. In: Third international congress on chemistry for cultural heritage; 2014; Vienna, Austria.
41. Loh W-Y. Classification and regression trees. Wiley Interdisc Rev. 2011;1(1):14–23.
42. Breiman L. Classification and regression trees. New York: Routledge; 1984. p. 368.
43. Larsen R. Microanalysis of parchment. London: Archetype; 2002. p. 180.